A Thermoreversible and Proton-Induced Gel−Sol Phase Transition with Remarkable Fluorescence Variation

ARTICLE *in* CHEMISTRY OF MATERIALS · OCTOBER 2008

Impact Factor: 8.35 · DOI: 10.1021/cm8019186

3 AUTHORS, INCLUDING:

Jong Won Chung
Samsung Advanced Institute of Technology
45 PUBLICATIONS **1,257** CITATIONS
SEE PROFILE

Byeong-Kwan An
Catholic University of Korea
46 PUBLICATIONS **2,741** CITATIONS
SEE PROFILE

A Thermoreversible and Proton-Induced Gel−Sol Phase Transition with Remarkable Fluorescence Variation

Jong Won Chung, Byeong-Kwan An, and Soo Young Park*

Department of Materials Science and Engineering ENG 445, Seoul National University, San 56-1, Shillim-dong, Kwanak-ku, Seoul 151-744, Korea

Received July 14, 2008. Revised Manuscript Received September 21, 2008

We have synthesized a novel highly fluorescent organogel system that uses a functional molecule with aggregation-induced enhanced emission (AIEE) properties. This AIEE organo gelator is more advanced than previously reported fluorescent gelators because it is practically nonfluorescent in the molecular sol state but highly fluorescent in the gel state, with a 170-fold enhancement in fluorescence intensity. This "functional fluorescent gelator" molecule forms strongly fluorescent and self-assembled gels in both nonpolar and polar protic solvents, even at low concentrations on the order of 0.2 wt %. These self-assembled organogels undergo completely thermoreversible and proton-induced gel-to-sol phase transitions with concomitant fluorescence intensity modulations. Moreover, we have demonstrated selective spatial patterning using the gel-to-sol transition with this organogel system.

Introduction

Gels derived from low-molecular-mass organic gelators (LMOGs) with π-conjugated molecular structure have attracted considerable interest in recent years because the π-conjugated nature of organogel networks is promising for applications in optoelectronic devices, template syntheses, and biomimetic systems.[1−8] Although the formation of an organogel from small organic molecules is an excellent example of a supramolecular self-assembly process, most LMOGs have been found by serendipity rather than design, and many aspects of organogels are still poorly understood. The control of gelation behavior induced by small molecules and the design of new organo gelators are therefore challenging goals that have led to a fascinating new field of organic materials. In particular, stimuli-responsive organogels[9−11] exhibit reversible changes in morphology and/or physical properties in response to various external stimuli and are drawing considerable attention because of their potential applications in chemical valves, drug delivery systems, sensors, and switches.[11−19] We have been especially interested in "functional fluorescent gels," which exhibit simultaneous gel-to-sol phase transitions with remarkable variation in fluorescence in response to temperature changes and/or photoacids and can be used in novel fluorescence patterning and imaging applications. Even though several fluorescent gel systems such as the cholesterol-functionalized 1,10-phenanthroline gelator[20] have been demonstrated that exhibit stimuli-sensitive fluorescence changes, these fluorescence changes are due to protonation and are not associated with the gel-to-sol phase transition.

The design of stimuli-responsive fluorescent gelators satisfying this definition is very complicated and has thus only rarely been reported: the single gelator molecule has to be capable of both gelation and fluorescence emission, which must also be reversibly and repeatedly modulated in morphology and/or physical properties by external stimuli such as temperature changes or light illumination. In the present study, we sought to develop an organo gelator with significant fluorescence variation. Among the many fluorescent organo gelators reported so far,[21−25] 1-cyano-trans-1,2-bis-(3′,5′-bis-trifluoromethyl-biphenyl) ethylene (CN-TFMBE,

* To whom correspondence should be addressed. E-mail: parksy@snu.ac.kr. Fax: (82)2-886-8331. Tel: (82)2-880-8347.

(1) Terech, P.; Weiss, R. G. *Chem. Rev.* **1997**, *97*, 3133–3159.
(2) Tanaka, T *Phys. Rev. Lett.* **1978**, *40*, 820–823.
(3) Hachisako, H.; Ihara, H.; Kamiya, T.; Hirayama, C.; Yamada, K. *Chem. Commun.* **1997**, 19–20.
(4) de Loos, M.; van Esch, J.; Stokroos, I.; Kellogg, R. M.; Feringa, B. L. *J. Am. Chem. Soc.* **1997**, *119*, 12675–12676.
(5) Sohna, J. E. S.; Fages, F. *Chem. Commun.* **1997**, 327–328.
(6) Shirakawa, M.; Fujita, N.; Tani, T.; Kaneko, K.; Ojima, M.; Fujii, A.; Ozaki, M.; Shinkai, S. *Chem.−Eur. J.* **2007**, *13*, 4155–4162.
(7) Sagawa, T.; Fukugawa, S.; Yamada, T.; Ihara, H. *Langmuir* **2002**, *18*, 7223–7228.
(8) de Loos, M.; van Esch, J.; Kellogg, R. M.; Feringa, B. L. *Angew. Chem., Int. Ed.* **2001**, *40*, 613–616.
(9) Stupp, S. I.; LeBonheur, V.; Walker, K.; Li, L. S.; Huggins, K. E.; Keser, M.; Amstutz, A. *Science* **1997**, *276*, 384–389.
(10) Muthukumar, M.; Ober, C. K.; Thomas, E. L. *Science* **1997**, *277*, 1225–1232.
(11) Sangeetha, N. M.; Maitra, U. *Chem. Soc. Rev.* **2005**, *34*, 821–836.
(12) van Esch, J. H.; Feringa, B. L. *Angew. Chem., Int. Ed.* **2000**, *39*, 2263–2266.
(13) Yagai, S.; Iwashima, T.; Kishikawa, K.; Nakahara, S.; Karatsu, T.; Kitamura, A. *Chem.−Eur. J.* **2006**, *12*, 3984–3994.
(14) Eastoe, J.; Sanchez-Dominguez, M.; Wyatt, P.; Heenan, R. K. *Chem. Commun.* **2004**, 2608–2609.
(15) Kato, T.; Hirai, Y.; Nakaso, S.; Moriyama, M. *Chem. Soc. Rev.* **2007**, *36*, 1857–1867.
(16) Tong, X.; Zhao, Y.; An, B. K.; Park, S. Y. *Adv. Funct. Mater.* **2006**, *16*, 1799–1804.
(17) Yang, Z. M.; Liang, G. L.; Xu, B. *Soft Mater.* **2007**, *3*, 515–520.
(18) Ajayaghosh, A.; Praveen, V. K.; Vijayakumar, C. *Chem. Soc. Rev.* **2008**, *37*, 109–122.
(19) Suzuki, T.; Shinkai, S.; Sada, K. *Adv. Mater.* **2006**, *18*, 1043–1046.
(20) Sugiyasu, K.; Fujita, N.; Takeuchi, M.; Yamada, S.; Shinkai, S. *Org. Biomol. Chem.* **2003**, *1*, 895–899.

10.1021/cm8019186 CCC: $40.75
Published on Web 10/22/2008

Scheme 1. Molecular Structures of the AIEE Organo Gelators

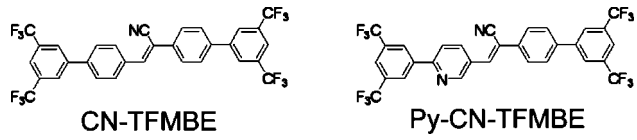

shown on the left of Scheme 1) is the most exciting, because it is practically nonfluorescent in the molecular sol state but is highly fluorescent in the gel state, with a more than 100-fold enhancement in fluorescence intensity.[21] To add "stimuli-responsive" properties to this high performance turn-on fluorescence gelator, we decided to modify its aromatic structure by including a photoacid-active pyridine unit, which results in the novel molecular structure 2-(3′,5′-bis(trifluoromethyl)biphenyl-4-yl)-3-(6-(3,5-bis(trifluoromethyl)phenyl) pyridin-3-yl)acrylonitrile (Py-CN-TFMBE, shown on the right of Scheme 1). The strategy of using pyridine rings as specific stimuli-responsive units in simultaneous self-assembly and fluorescence modulation has previously been exploited for the array patterning of fluorescent organic nanoparticles.[26]

Experimental Section

Materials. All commercially available reagents were purchased from Alfa Aesar Co. and Sigma Aldrich Chemical Co and used without further purification unless otherwise stated.

Synthesis of 6-(3,5-Bis(trifluoromethyl)phenyl)pyridine-carboxaldehyde (1). 6-Bromo-3-pyridinecarboxaldehyde (0.5 g, 2.69 mmol), 3,5-bis(trifluoromethyl)phenylboronic acid (0.76 g, 2.95 mmol) and tetrakis(triphenylphosphine)palladium(0) (0.02 g, 0.004 mmol) were dissolved in 24 mL of tetrahydrofuran. After addition of 8 mL of aqueous 2 N potassium carbonate solution, the reaction mixture was stirred at 80 °C and refluxed for 100 h. The cooled crude mixture was poured onto 100 mL of water and extracted with ethyl acetate (80 mL) and dried over anhydrous magnesium sulfate. Finally silica gel column chromatography (*n*-hexane: EtOAc = 7: 1) gave a white powder (0.71 g, 2.22 mmol) in 82.5% yield. ^{1}H NMR ($CDCl_3$, 300 MHz): δ 10.20 (s, 1H, formyl), 9.20 (s, 1H, Ar−H), 8.58 (s, 2H, Ar−H), 8.33 (d, 1H, Ar−H), 8.02 (d, 1H, Ar−H), 8.00 (s, 1H, Ar−H); ^{13}C NMR($CDCl_3$, 125 MHz): δ 121.03, 123.90, 127.75, 131.09, 132.59, 132.86, 137.47, 140.13, 152.56, 158.80, 190.27; Anal. Calcd for $C_{14}H_7F_6NO$: C, 52.68; H, 2.21; N, 4.39. Found: C, 52.70; H, 2.22; N, 4.37.

Synthesis of 2-(3′,5′-Bis(trifluoromethyl)biphenyl-4-yl)acetonitrile (2). This compound was synthesized according to the method described in our previous paper.[21] A white powder was obtained in 79% yield. ^{1}H NMR ($CDCl_3$, 300 MHz): δ 7.99 (s, 2H, Ar−H), 7.88 (s, 1H, Ar−H), 7.64 (d, 2H, Ar−H), 7.49 (d, 2H, Ar−H), 3.84 (s, 2H, vinyl). ^{13}C NMR($CDCl_3$, 125 MHz): δ 23.60, 117.62, 121.52, 127.37, 128.22, 129.10, 130.97, 132.39, 132.65, 138.38, 142.54; Anal. Calcd for $C_{16}H_9F_6N$: C, 58.37; H, 2.76; F, 34.62; N, 4.25. Found: C, 58.49; H, 2.86; F, 34.40; N, 4.25.

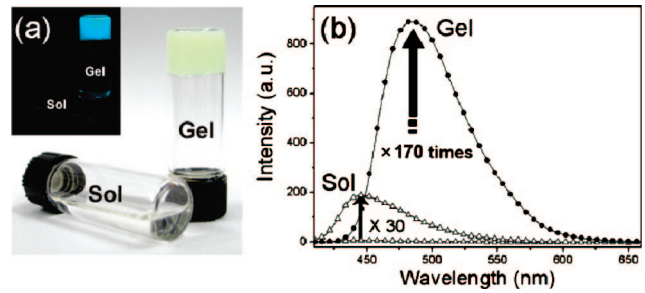

Figure 1. (a) Gel and sol states of Py-CN-TFMBE. The photograph in the inset shows the fluorescence emissions of the sol and gel states of Py-CN-TFMBE (under a 365 nm UV lamp). (b) PL spectra of Py-CN-TFMBE in the sol and gel states. The enhancement in fluorescence intensity (170-fold) was calculated from the integral areas of the PL spectra.

Synthesis of 2-(3′,5′-Bis(trifluoromethyl)biphenyl-4-yl)-3-(6-(3,5-bis(trifluoromethyl)phenyl) pyridin-3-yl)acrylonitrile (Py-CN-TFMBE). A mixture of 2-(3′,5′-bis(trifluoromethyl)biphenyl-4-yl)acetonitrile (0.49 g, 1.49 mmol) and 6-(3,5-bis(trifluoromethyl)phenyl)pyridinecarboxaldehyde (0.48 g, 1.49 mmol) in tert-butyl alcohol (15 mL) and THF (1 mL) was stirred at 50 °C for 1 h. Tetrabutylammonium hydroxide (TBAH) (1 M solution in methanol) (0.16 mL) was slowly dropped into the mixture and stirred for 1 h. The resulting green precipitate was collected by filtration and washed with methanol. Finally, silica gel column chromatography gave a greenish yellow powder in 71% yield. mp 272−273 °C. ^{1}H NMR ($CDCl_3$, 300 MHz) δ 9.02 (s, 1H, Ar−H), 8.68 (d, 1H, Ar−H), 8.57 (s, 2H, Ar−H), 8.06 (s, 2H, Ar−H), 7.99 (d, 2H, Ar−H), 7.90 (s, 1H, Ar−H), 7.88 (d, 2H, Ar−H), 7.75 (d, 2H, Ar−H), 7.68 (s, 1H, vinyl). ^{13}C NMR($CDCl_3$, 125 MHz): δ 114.12, 117.37, 120.75, 121.668, 123.40, 125.30, 127.23, 127.35, 128.31, 129.62, 132.41, 132.85, 134.40, 136.26, 137.93, 139.86, 140.36, 142.11, 151.97, 155.40. MS(FAB) (*m*/*z*): calcd for $C_{30}H_{14}F_{12}N_2$, 630; found, 630. Anal. Calcd for $C_{30}H_{14}F_{12}N_2$: C, 57.16; H, 2.24; N, 4.44. Found: C, 57.29; H, 2.22; N, 4.37.

Nanosuspension Preparation. A nanoparticle suspension was prepared by a simple reprecipitation method.[27] Distilled water was slowly injected into a THF solution of Py-CN-TFMBE with vigorous stirring at room temperature, using a syringe pump. Before injection of the distilled water, both the distilled water and the Py-CN-TFMBE solution were filtered through a membrane filter of pore size 0.2 μm. The FE-SEM image of the Py-CN-TFMBE nanoparticles shown in Figure 4c was obtained by dropping a Py-CN-TFMBE nanoparticle suspension onto a slide glass.

Measurement of Gel Melting Temperature. The gel melting temperature was measured by the "dropping ball method". A metal ball (440 mg) was placed over the Py-CN-TFMBE gel in the vial. The gel sample was immersed in a temperature-regulated bath, and the position of the ball was observed while the temperature was increased at 1 °C min^{-1}. The gel melting temperature was determined as the temperature when the ball reached the bottom of the vial.

Irradiation Procedure for the Gel−Sol Phase Transition. Py-CN-TFMBE/PAG organogel in a rectangular quartz cell (path length, 1.0 mm) was placed ca. 10 cm from a 254 nm hand-held UV lamp (1.2 mW cm^{-2}) and irradiated under atmospheric conditions at room temperature for 30 min.

Instrumentation. UV−visible absorption spectra were recorded on a Shimadzu UV-1650 PC spectrometer from 250 to 700 nm in 0.2 nm increments. The fluorescence emission spectra were obtained using a Shimadzu RF 5301 PC spectrofluorophotometer. Differential scanning calorimetry (DSC) was performed on a Perkin-Elmer

(21) An, B. K.; Lee, D. S.; Lee, J. S.; Park, Y. S.; Song, H. S.; Park, S. Y. *J. Am. Chem. Soc.* **2004**, *126*, 10232–10233.
(22) Hulvat, J. F.; Sofos, M.; Tajima, K.; Stupp, S. I. *J. Am. Chem. Soc.* **2005**, *127*, 366–372.
(23) Bao, C. Y.; Lu, R.; Jin, M.; Xue, P. C.; Tan, C. H.; Xu, T. H.; Liu, G. F.; Zhao, Y. Y. *Chem.−Eur. J.* **2006**, *12*, 3287–3294.
(24) Yang, X. C.; Lu, R.; Xu, T. H.; Xue, P. C.; Liu, X. L.; Zhao, Y. Y. *Chem. Commun.* **2008**, 453–455.
(25) Kumar, N. S. S.; Varghese, S.; Narayan, G.; Das, S. *Angew. Chem., Int. Ed.* **2006**, *45*, 6317–6321.
(26) An, B. K.; Kwon, S. K.; Park, S. Y. *Angew. Chem., Int. Ed.* **2007**, *46*, 1978–1982.

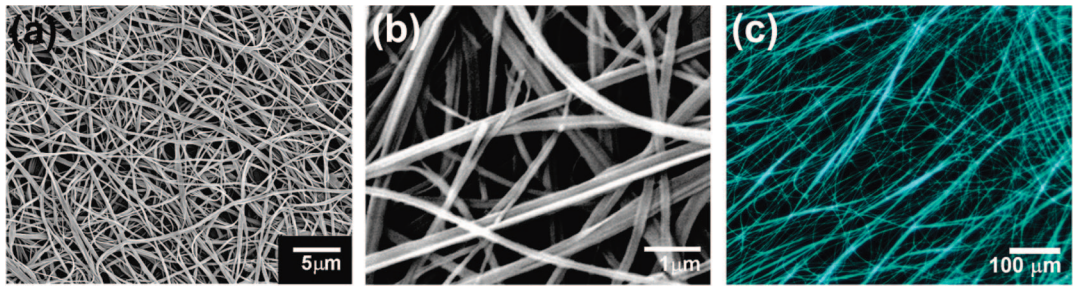

Figure 2. SEM images of the dried organogel state of Py-CN-TFMBE in 1,2-dichloroethane (0.8 wt %) at magnifications of (a) 3000 and (b) 20 000, and (c) fluorescence microscopy image of a Py-CN-TFMBE organogel.

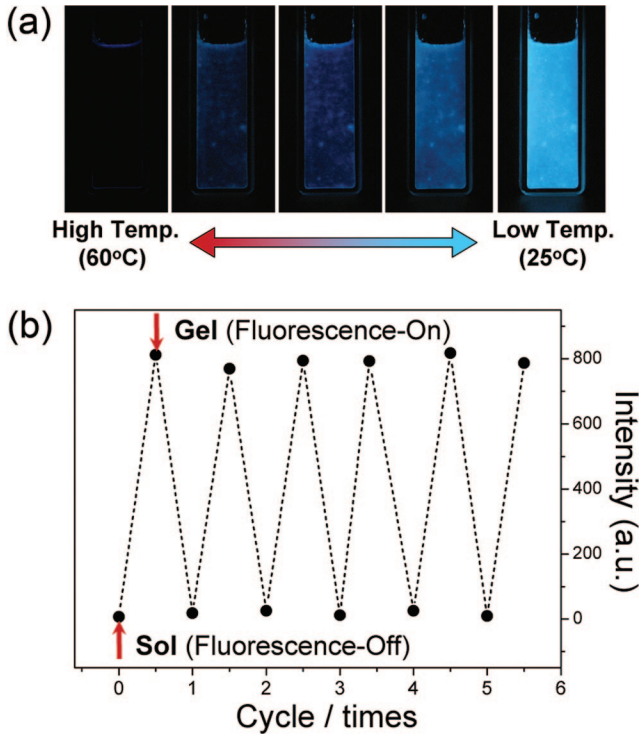

Figure 3. (a) Fluorescence images of Py-CN-TFMBE for various temperatures. (b) The fluorescence modulation spectrum shows the thermoreversibility of the PL intensity of the gel and sol states.

DSC7 at a heating rate of 10 °C min^{-1}. ^1H NMR spectra were recorded on a DPX Bruker 300 (300 MHz). All NMR spectra were referenced to the solvent. ^{13}C NMR spectra were measured using a Bruker Avance 500 (500 MHz) spectrometer. Proton (0.1 ppm) chemical shifts were measured with respect to internal TMS in $CDCl_3$. ^{13}C chemical shifts were recorded in ppm relative to $CDCl_3$. TLC analyses were carried out on aluminum sheets coated with silica gel 60 (Merck 5554). Column chromatography was performed on Merck silicagel 60. Mass spectra were measured using a JEOL, JMS AX505WA mass spectrometer. Elemental analysis was carried out using a CE Instruments EA110 elemental analyzer. Field Emission Scanning Electron Microscopy (FE-SEM) images were obtained with a JSM-6330F (JEOL) FE-SEM at an acceleration voltage of 12 kV, after sputter deposition of a thin conductive platinum coating onto the films. Fluorescence images were obtained using a digital camera (Nikon-Coolpix 995) and a microscope (Leica) under illumination at 365 nm.

(27) Chung, H. R.; Kwon, E.; Kawa, H.; Kasai, H.; Nakanishi, H. *J. Cryst. Growth* **2006**, *294*, 459–463.

Results and Discussion

Synthesis. Scheme 1 shows the molecular structures of the fluorescent organo gelators.The functional organo gelator containing the pyridyl moiety, i.e., 2-(3′,5′-bis(trifluoromethyl) biphenyl-4-yl)-3-(6-(3,5-bis(trifluoro-methyl)phenyl)pyridin-3-yl) acrylonitrile (compound 3, Py-CN-TFMBE), was conveniently synthesized according to Scheme 2 The two biphenyl compounds, **1** and **2**, were synthesized by using the Suzuki coupling reaction of an aromatic boronic acid and an aromatic bromide. Compounds **1** and **2** were then reacted via a tetrabutylammonium hydroxide (TBAH) catalyzed Knoevenagel condensation to give the crude product 3. The green precipitate was collected by filtration and washed with methanol. Finally, compound **3** was purified as a greenish yellow powder by carrying out silica gel column chromatography with dichloromethane (DCM) eluent (yield = 71%). CN-TFMBE (see Scheme 1 for the structure) was also synthesized as a "non-stimuli-responsive" analog of **3**. The compounds were identified with ^1H NMR, ^{13}C NMR, and MS spectral evidence and elemental analyses.

Gelation and Fluorescence Properties of Py-CN-TFMBE. As expected, Py-CN-TFMBE forms a highly fluorescent organogel in organic solution that is much the same as that of CN-TFMBE.[21] The organogel is prepared by dissolving Py-CN-TFMBE (0.8 wt/vol %) in 1,2-dichloroethane with gentle heating (Figure 1a, left vial), followed by slow cooling to room temperature. The gel formation during cooling of Py-CN-TFMBE is accompanied by a drastic increase in the fluorescence intensity, as shown in Figure 1b. The gel is opaque, and exhibits no gravitational flow (Figure 1a, right vial) and strong fluorescence (Figure 1a, inset photograph). The field emission scanning electron microscopy (FE-SEM) and fluorescent microscopy images of the dried gel shown in Figure 2 indicated that the Py-CN-TFMBE gel consists of very long and entangled fibers of fluorescent fibrous aggregates that stabilize the gel state. Although Py-CN-TFMBE in solution and in the melt state is almost nonfluorescent, its gel exhibits strong fluorescence, with an enhancement in fluorescence intensity by a factor of more than 170 (Figure 1b).

The results of the gelation tests and the critical gel concentrations (CGCs) are summarized in Table 1. The gelation behavior of Py-CN-TFMBE in various organic solvents was investigated by using the "stable inversion in

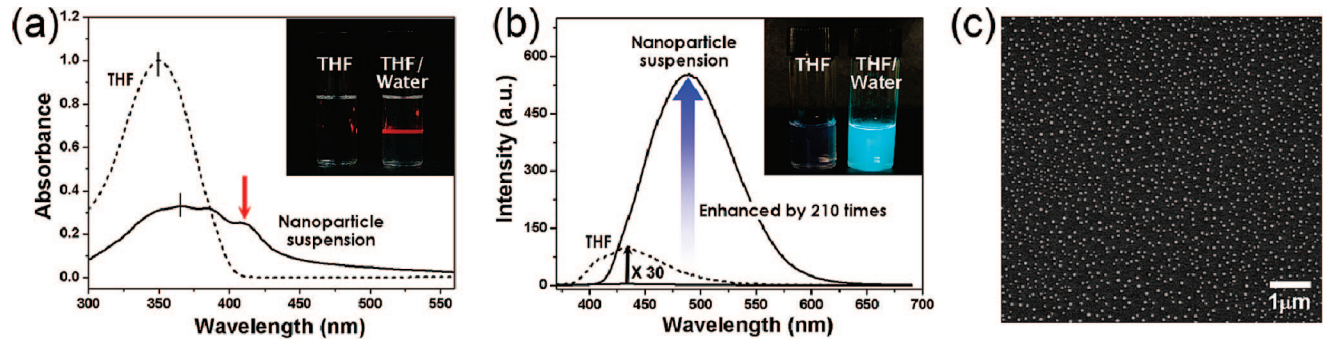

Figure 4. UV−vis/PL spectra of Py-CN-TFMBE (2×10^{-5} mol L^{-1}) in THF and in colloidal nanosuspension (2×10^{-5} mol L^{-1}) (60 wt % water addition in THF solution). (a) UV−vis absorption spectra. Inset: photograph showing light scattering in the nanosuspension. (b) The PL spectra. PL intensities were normalized according to the corresponding UV absorbance. The inset photographs show the fluorescence emission from a Py-CN-TFMBE solution (left vial) and the colloidal nanosuspension (right vial) under 365 nm UV light. (c) SEM image of the colloidal nanosuspension.

Scheme 2. Synthesis of the Py-CN-TFMBE Organo Gelator[a]

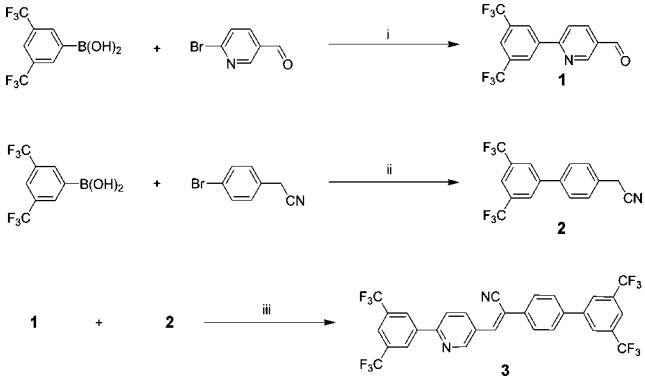

[a] (i−ii) Suzuki coupling reaction: $Pd(PPh_3)_4$, THF/2N K_2CO_3 aq. at 80 °C for 100 h (i) and overnight (ii). (iii) Knoevenagel condensation: tert-butanol/THF, TBAH at 50 °C for 1 h.

Table 1. Gelation Behavior and CGCs of Py-CN-TFMBE in Various Organic Media

solvent	phase[a] (CGC)[b]	solvent	phase[a] (CGC)[b]
cyclohexane	G (0.3)	ethylacetate	S
n-hexane	G (0.3)	ethanol	G (0.2)
benzene	G (0.8)	methanol	G (0.2)
toluene	G (0.8)	1,2-dichloroethane	G (0.4)
tetrahydrofuran	S	1,2,3,4-tetrachloroethane	G (0.4)
chloroform	PG (0.8)	DMF	S
dichloromethane	S	DMSO	S
acetonitrile	G (0.2)		

[a] The solution was warmed until Py-CN-TFMBE was dissolved and then cooled to 25 °C to produce the gel (G, stable gel; PG, partial gel; S, soluble). [b] The critical gelation concentration (wt %) is the minimum concentration necessary for gelation.

a test tube" method.[28] A highly fluorescent organogel was formed when a mixture of Py-CN-TFMBE and an organic solvent were heated to form a homogeneous fluid and then allowed to cool at 25 °C. As summarized in Table 1, we found that Py-CN-TFMBE has strong gelation capabilities in both polar and nonpolar solvents. The formation of fluorescent gels in nonpolar solvents, such as cyclohexane, hexane, benzene, and toluene, was found to occur within one minute after a hot solution was placed in room temperature surroundings, with CGCs as low as 0.8 wt %. Of the polar solvents, gelation was also observed in methanol, ethanol, chloroform, acetonitrile, 1,2-dichloroethane, and 1,2,3,4-tetrachloroethane but not in ethyl acetate, tetrahydrofuran, DMF and DMSO, or DMF. The formation of a self-assembled Py-CN-TFMBE organogel was found to be completely thermo-reversible in the organic solvents. The gel-to-sol phase transition temperature (T_{gel}) for the 1,2-dichloroethane gel (0.8 wt %) was estimated to be 59−61 °C by using the ball dropping method. The gelator was found to be initially insoluble in these solvents at room temperature, but the mixtures became clear after gentle heating. Upon cooling of these solutions to room temperature, the formation of immobile gels was observed. This thermoreversible gelation process is characteristically accompanied by enhanced fluorescence emission (panels a and b in Figure 3).

The remarkable fluorescence enhancement in the Py-CN-TFMBE gel can be unambiguously explained in terms of the phenomenon of aggregation-induced enhanced emission (AIEE),[26,29−34] which occurs for a special class of molecules that includes CN-TFMBE.[21] In principle, the AIEE effect is observed in molecules with "elastic twists," i.e., in molecules that are prone to large conformational changes in response to specific intermolecular interactions, via external stimuli such as temperature and pressure changes, or exposure to solvent vapor. Isolated Py-CN-TFMBE molecules in dilute solution are significantly twisted by the internal steric interactions between the biphenyl units and the bulky cyano groups attached to the vinylene moiety, which generally suppresses the radiative decay channel and renders the solution nonfluorescent, as shown in Figure 4b. However, in the condensed state, as for colloidal nanoparticles of Py-CN-TFMBE, the strong intermolecular $\pi-\pi$ interactions and the subtle balance of the polar and bulky cyano groups cooperatively induce molecular planarization and *J*-type

(28) Jeong, B.; Bae, Y. H.; Kim, S. W. *Macromolecules* **1999**, *32*, 7064–7069.
(29) An, B. K.; Kwon, S. K.; Jung, S. D.; Park, S. Y. *J. Am. Chem. Soc.* **2002**, *124*, 14410–14415.
(30) Luo, J. D.; Xie, Z. L.; Lam, J. W. Y.; Cheng, L.; Chen, H. Y.; Qiu, C. F.; Kwok, H. S.; Zhan, X. W.; Liu, Y. Q.; Zhu, D. B.; Tang, B. Z. *Chem. Commun.* **2001**, 1740–1741.
(31) Li, Y. P.; Li, F.; Zhang, H. Y.; Xie, Z. Q.; Xie, W. J.; Xu, H.; Li, B.; Shen, F. Z.; Ye, L.; Hanif, M.; Ma, D. G.; Ma, Y. G. *Chem. Commun.* **2007**, 231–233.
(32) Han, M.; Hara, M. *J. Am. Chem. Soc.* **2005**, *127*, 10951–10955.
(33) Kim, S.; Zheng, Q.; He, G. S.; Bharali, D. J.; Pudavar, H. E.; Baev, A.; Prasad, P. N. *Adv. Funct. Mater.* **2006**, *16*, 2317–2323.
(34) Ning, Z. J.; Chen, Z.; Zhang, Q.; Yan, Y. L.; Qian, S. X.; Cao, Y.; Tian, H. *Adv. Funct. Mater.* **2007**, *17*, 3799–3807.

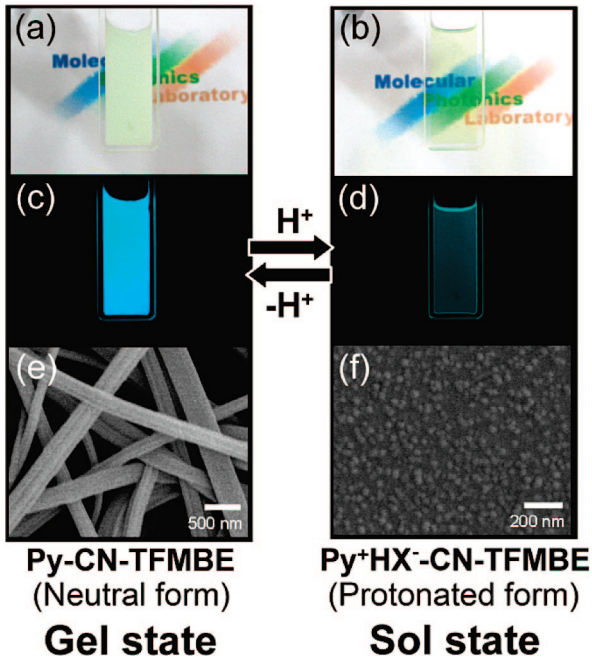

Figure 5. (a, b) Photographs of the reversible phase transition between the gel and sol states of Py-CN-TFMBE/PAG in 1,2-dichloroethane (neutral gel (a) and protonated sol (b)). (c, d) Fluorescence images and (e, f) SEM images of the neutral gel and the protonated sol, respectively.

aggregate stacking, as indicated by the red-shifted absorption (maximum peaks from 350 to 366 nm) and *J*-band (red arrow) respectively, as shown in Figure 4. Concomitant with this planarization and *J*-type stacking of Py-CN-TFMBE, the fluorescence intensity increases by a factor of 210.

Proton-Induced Gel−Sol Phase Transition. The "stimuli-responsive" feature of Py-CN-TFMBE that distinguishes it from other AIEE dyes is the presence of the pyridine ring, which can be readily protonated and thus Py-CN-TFMBE forms bulky quaternary salts with counterpart ions via photochemical reactions.[35−37] This protonation process is expected to result in the deterioration of the self-assembled gel state with concomitant changes in the fluorescence intensity. To demonstrate the proton-induced gel-to-sol transition of Py-CN-TFMBE, we prepared a fluorescent organogel in a rectangular quartz cell (1.0 mm path length) by cooling a Py-CN-TFMBE (0.8 wt/vol %) solution in 1,2-dichloroethane, into which was added a photoacid generator (PAG, triphenylsulfonium trifluoromethane sulfonate, $\lambda_{max,abs}$ = 250 nm) (3 equiv. of Py-CN-TFMBE) that releases protons (H^+) and counterions ($X^- = CF_3SO_3^-$) upon UV light exposure.

Similar to the pure Py-CN-TFMBE gel system, the Py-CN-TFMBE/PAG solution in the rectangular quartz cell is very transparent and almost nonfluorescent before gelation; an opaque and highly fluorescent Py-CN-TFMBE/PAG gel is reversibly generated upon cooling due to the formation of entangled 3D networks consisting of bundles of Py-CN-TFMBE fibrous aggregates and the resulting AIEE effect (shown on the left of Figure 5). This opaque organogel is completely converted to a transparent yellow-green sol with

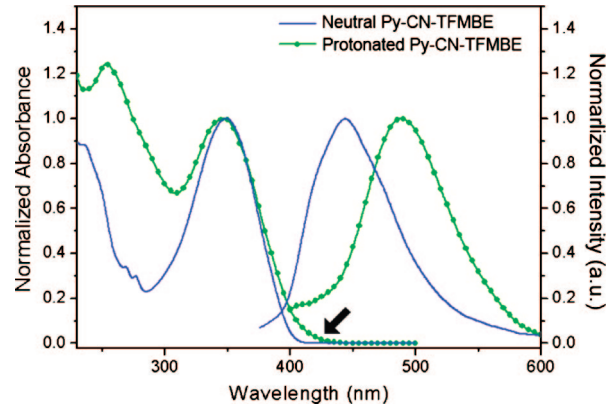

Figure 6. UV−vis absorption and PL spectra of Py-CN-TFMBE in solution state with a PAG (blue line, neutral Py-CN-TMBE) and those after 254 nm UV light illumination for 1 min (green line, protonated Py-CN-TFMBE). The arrow indicates the cutoff wavelength of the UV absorption spectra.

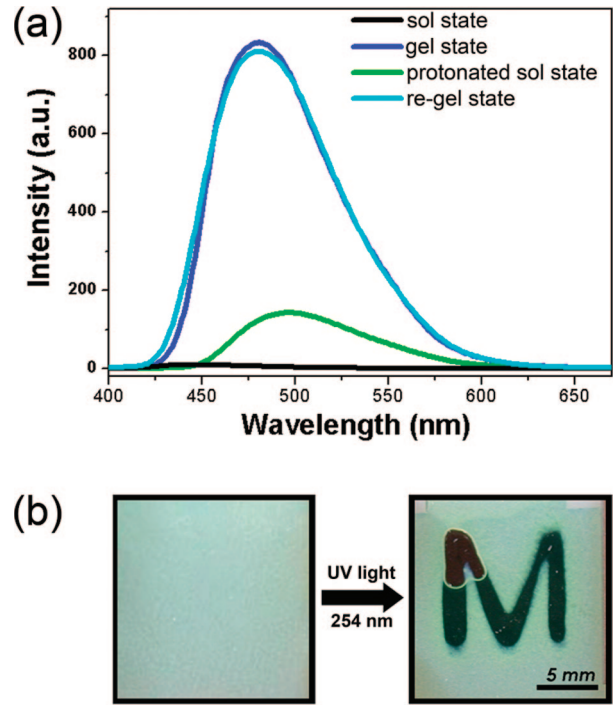

Figure 7. (a) Fluorescence spectra of Py-CN-TFMBE/PAG in the neutral sol state, neutral gel state, protonated sol state, and reneutral gel state. (b) A photograph of the initial gel state (left) and a spatial patterning image of the letter "M" (right); the background is a blackboard.

a significantly decreased fluorescence emission when it is irradiated with 254 nm UV light for 30 min (see the right of Figure 5). This result implies that the fibrous Py-CN-TFMBE aggregates in the Py-CN-TFMBE/PAG gel are effectively disassembled as a result of the protonation of the pyridine rings by the photochemically generated photoacids. The SEM images in Figure 5f show the morphology of the fibrous aggregates after disassembly by protonation.

This gel-to-sol phase transition is not the result of any other photoreaction such as photodimerization, isomerization, or branching in aggregate states, because when a Py-CN-TFMBE organogel without PAG was irradiated with 254 nm UV light for several hours, no gel-to-sol phase transition, fluorescence changes, or ^{1}H NMR proton shift occurred. The protonation of the pyridine rings in the Py-CN-TFMBE molecules was confirmed by examination of the changes in

(35) McQuade, D. T.; Pullen, A. E.; Swager, T. M. *Chem. Rev.* **2000**, *100*, 2537–2574.
(36) Fu, D. K.; Xu, B.; Swager, T. M. *Tetrahedron* **1997**, *53*, 15487–15494.

the ^{1}H NMR and optical spectra. In the ^{1}H NMR spectrum of Py-CN-TFMBE, the proton peaks due to the pyridine ring are shifted from 9.02 and 8.68 ppm to 9.44 and 9.38 ppm upon protonation. The UV−vis absorption peak and the λ_{max} of the PL spectrum of the protonated Py-CN-TFMBE sol state are red-shifted by 10 and 44 nm respectively, due to the optical band gap narrowing induced by intramolecular charge transfer upon protonation of the pyridyl units[36,37] (see Figure 6). The disassembly of the fibrous Py-CN-TFMBE aggregates in the protonated Py-CN-TFMBE sol state was also confirmed by monitoring the disappearance of the 415 nm shoulder band in the UV−vis absorption spectrum; this *J*-type band is due to Py-CN-TFMBE aggregates. Note also that the fluorescence intensity decreases to 1/6 of its original value, which is due to the loss of the AIEE effect (see Figure 7a).

The selective spatial patterning of the gel-to-sol transition with relevant fluorescence modulation is shown in Figure 7b for an illumination of 254 nm through a photomask. More interestingly, the protonated Py-CN-TFMBE sol state is completely restored to a strongly fluorescent gel state when triethylamine (15 μL) is added to deprotonate the pyridine rings.

Conclusion

We have prepared a novel stimuli-responsive π-conjugated fluorescent organo gelator (Py-CN-TFMBE) and investigated its supramolecular assembly and fluorescence properties that arise during its gel-to-sol phase transition. Py-CN-TFMBE forms highly fluorescent organogels in various organic solvents, with critical gel concentrations as low as 0.2 wt %. Fluorescence photopatterning of a Py-CN-TFMBE gel was successfully demonstrated by using the proton-induced gel-to-sol phase transition with concomitant change in fluorescence.

Acknowledgment. This work was supported by the Korea Science and Engineering Foundation (KOSEF) through the National Research Laboratory. Program funded by the Ministry of Science and Technology (No.2006-03246).

Supporting Information Available: Molecular characteristics and experimental details (PDF). This material is available free of charge via the Internet at http://pubs.acs.org.

CM8019186

(37) Scheiner, S.; Kar, T. *J. Phys. Chem. B* **2002**, *106*, 534–539.